Available online at www.sciencedirect.com

SCIENCE DIRECT

Virology 336 (2005) 291 – 298

VIROLOGY

www.elsevier.com/locate/yviro

Functional characterization of Ebola virus L-domains using VSV recombinants

Takashi Irie, Jillian M. Licata, Ronald N. Harty*

Department of Pathobiology, School of Veterinary Medicine, University of Pennsylvania, 3800 Spruce Street, Philadelphia, PA 19104-6049, USA

Received 31 January 2005; returned to author for revision 23 February 2005; accepted 23 March 2005
Available online 19 April 2005

Abstract

VSV recombinants containing the overlapping L-domain sequences from Ebola virus VP40 (PTAPPEY) were recovered by reverse-genetics. Replication kinetics of M40-WT, M40-P24L, and M40-Y30A were indistinguishable from VSV-WT in BHK-21 cells, whereas the double mutant (M40-P2728A) was defective in budding. Insertion of the Ebola L-domain region into VSV M protein was sufficient to alter the dependence on host proteins for efficient budding. Indeed, M40 recombinants containing a functional PTAP motif specifically incorporated endogenous tsg101 into budding virions and were dependent on tsg101 expression for efficient budding. Thus, VSV represents an excellent negative-sense RNA virus model for elucidating the functional aspects and diverse host interactions associated with the L-domains of Ebola virus.

Keywords: Ebola virus; L-domains; VSV recombinants

Introduction

The VP40 protein of Ebola virus plays a key role in driving assembly and budding of virions. Indeed, VP40 will bud from mammalian cells in the form of a virus-like particle (VLP) in the absence of other viral proteins (Harty et al., 2000; Jasenosky and Kawaoka, 2004; Kolesnikova et al., 2002; Licata et al., 2003; Martin-Serrano et al., 2001; Noda et al., 2002; Panchal et al., 2003; Timmins et al., 2001). However, budding of VP40-containing VLPs, as well as VLPs of other negative-sense RNA viruses, is most efficient in the presence of additional viral proteins including GP and NP (Licata et al., 2004; Noda et al., 2002; Schmitt and Lamb, 2004; Schmitt et al., 2002; Swenson et al., 2004). In addition to viral proteins, host proteins such as tsg101 and other components of the ESCRT machinery have been shown to play an important role in facilitating efficient release of VP40 VLPs (Irie et al., 2004b; Licata et al., 2003; Martin-Serrano et al., 2001; Timmins et al., 2003; von Schwedler et al., 2003). Host proteins contribute to the budding process through interactions with viral late (L) domains present in matrix or matrix-like proteins (Gottwein et al., 2003; Harty et al., 2001; Martin-Serrano et al., 2003; Ott et al., 2002; Perez et al., 2003; Puffer et al., 1997; Strack et al., 2003; von Schwedler et al., 2003). The VP40 protein is unique in that it possesses two overlapping L-domain motifs at its N-terminus. Both the PTAP and PPEY motifs of VP40 have been shown to possess L-domain activity in a VLP budding assay and mediate interactions with host proteins tsg101 and Nedd4, respectively (Harty et al., 2000; Licata et al., 2003; Timmins et al., 2003). The use of VP40 VLP budding assays has provided much useful information regarding the importance of the L-domain region to budding. However, to more accurately assess the role of the Ebola virus L-domain region during virus replication, we attempted to incorporate the L-domain region of VP40 including flanking amino acids into VSV using reverse-genetics. Our results indicate that the VP40 sequences possess L-domain activity in the context of the VSV M protein and a VSV infection. Each of the PTAP and PPEY motifs exhibited L-domain activity

* Corresponding author. Fax: +1 215 898 7887.
E-mail address: rharty@vet.upenn.edu (R.N. Harty).

0042-6822/$ - see front matter © 2005 Elsevier Inc. All rights reserved.
doi:10.1016/j.virol.2005.03.027

independently and each was capable of interacting with and packaging specific host proteins. For example, the presence of the Ebola virus PTAP motif altered the dependence of VSV on tsg101 expression for efficient budding. Thus, VSV represents an excellent model system for characterizing Ebola virus L-domain function and to elucidate the different pathways of budding directed by viral L-domains and host protein interactions.

Results

Recovery and growth kinetics of M40 recombinants

To address the function of Ebola virus L-domains and flanking sequences in the context of a virus infection, VSV recombinants containing Ebola virus L-domain sequences were recovered using a reverse-genetics approach (Fig. 1A). The M40-WT recombinant virus contains amino acids 6–20 from the N-terminus of the VP40 protein of Ebola virus (Zaire). In addition, three M40 mutants were recovered that possess mutations in either the $_{24}$PTAP$_{27}$ motif (M40-P24L), the $_{27}$PPEY$_{30}$ motif (M40-Y30A), or both motifs (M40-P2728A) (Fig. 1A). The corresponding sequences within the M protein of VSV-WT and the VSV PY > A4 mutant are shown for comparison (Fig. 1A). The PSAP region of VSV M (aa 33–44) remained unaltered in all recombinants, since we demonstrated previously that the PSAP motif does not have L-domain activity in BHK-21 cells (Fig. 1A) (Irie et al., 2004a).

Growth kinetics for all of the M40 recombinants were assessed by a one-step growth curve in BHK-21 cells (Fig. 1B). VSV-WT and the budding-defective PY > A4 mutant served as a positive and negative control, respectively (Fig. 1B). Our results indicated that the growth curves for M40-WT, M40-P24L, and M40-Y30A were virtually indistinguishable from that of VSV-WT (Fig. 1B). Thus, mutations that disrupted the PTAP motif alone or the PPEY motif alone did not result in a budding-defective virus in BHK-21 cells. This finding indicates that each Ebola virus L-domain motif possesses independent L-domain activity in the context of a VSV infection. In contrast, the M40-P2728A double mutant was defective in budding as demonstrated by titers at least 10-fold lower than those of M40-WT at various time points post-infection (Fig. 1B). Thus, titers of the budding-defective PY > A4 mutant resembled those of the L-domain-defective M40-P2728A mutant (Fig. 1B).

We next examined the virion protein profile, plaque area, and budding using electron microscopy for the M40 recombinants. The protein profiles of VSV-WT, PY>A4, M40-WT, M40-P24L, M40-Y30A, and M40-P2728A virions were compared by SDS–PAGE (Fig. 2A). As expected, the amount of virion proteins detected for the budding-defective PY > A4 mutant was reduced significantly from that of VSV-WT (Fig. 2A, lanes 1 and 2). Similarly, the amount of virion proteins detected for M40-P2728A was reduced significantly from that of M40-WT (compare lanes 3 and 6). The amount of virion proteins for the single mutants M40-P24L and M40-Y30A was virtually identical to that of M40-WT (compare lanes 3, 4, and 5). These

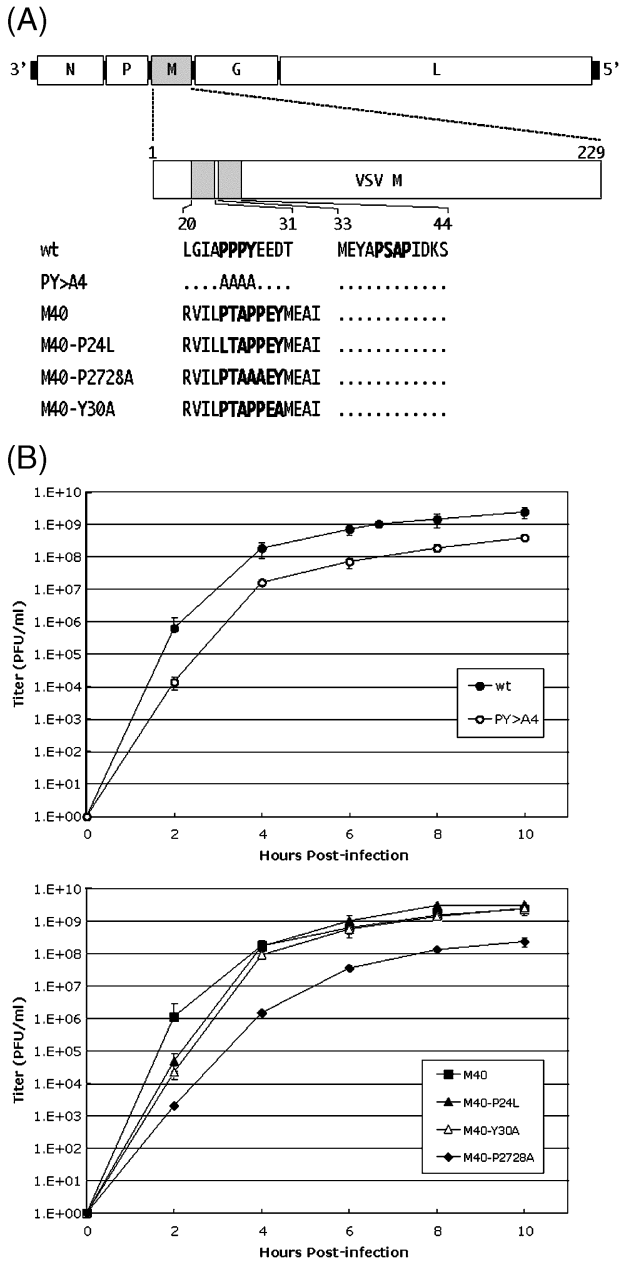

Fig. 1. Growth kinetics of M40 recombinant viruses. (A) Diagram of VSV genome with the M gene highlighted in grey. The VSV M gene (aa 1–229) is expanded and the sequences aa 20–31 and aa 33–44 are indicated. The dotted line indicates that the WT M sequence is maintained. The amino acid sequence within the L-domain region (20–31) is shown for VSV-WT, PY > A4 mutant, M40, M40-P24L, M40-P2728A, and M40-Y30A. (B) Graph of growth kinetics and titers of VSV-WT and PY > A4 at the indicated times post-infection of BHK-21 cells. The titers represent an average of at least 2 independent experiments. (C) Graph of growth kinetics and titers for M40, M40-P24L, M40-Y30A, and M40-P2728A at the indicated times post-infection of BHK-21 cells. The titers represent an average of at least 2 independent experiments.

results are consistent with the budding defect exhibited by PY > A4 and M40-P2728A in Fig. 1. Importantly, the amount of M protein synthesized from all VSV recombinants was identical in infected cell extracts (Fig. 2B). Thus, insertion of Ebola virus sequences into M did not affect protein synthesis or stability.

We next sought to determine whether the presence of the Ebola virus L-domain sequences in VSV M protein affected plaque size. The plaque areas formed by VSV-WT, PY > A4, and all of the M40 recombinant viruses on a monolayer of BHK-21 cells were measured (Fig. 2C). As shown previously, the plaque size of PY > A4 was approximately 2-fold smaller than that of VSV-WT (Fig. 2C) (Irie et al., 2004a; Jayakar et al., 2000). No significant difference was observed between the plaque size formed by VSV-WT and that formed by M40-WT (Fig. 2C). Similarly, average plaque areas formed by M40-P24L and M40-Y30A were indistinguishable from those of M40-WT, whereas M40-P2728A displayed a small-plaque phenotype similar to that of PY > A4 (Fig. 2C).

We next utilized electron microscopy to visualize budding virions. We predicted that the double mutant would display the characteristic membrane-tethered phenotype on the plasma membrane of infected cells. Indeed, relatively few budding virions of M40-WT, M40-P24L, and M40-Y30A were found tethered to the plasma membrane, whereas M40-P2728A was found predominantly tethered to the surface of the cell (Fig. 2D). Interestingly, M40-WT virions, and to a slightly lesser degree M40-P24L and M40-Y30A virions (data not shown), were observed on internal membranes and in intracellular vesicles (Fig. 2D).

The type of L-domain present directs packaging of host proteins into budding virions and dictates the pathway for efficient budding

The packaging of specific host proteins into budding VP40 VLPs has been reported by us previously (Licata et al., 2003). Incorporation of specific host proteins in budding VLPs is thought to be indicative of a biological function for these host proteins during the budding process. We sought to determine whether the M40 recombinants possessing different L-domain motifs would interact with and package distinct host proteins into infectious virus.

BHK-21 cells were infected with VSV-WT, PY > A4, or the M40 recombinants, and equivalent amounts of virions were harvested at 8 h post-infection. Antiserum against endogenous tsg101 was used to determine whether tsg101

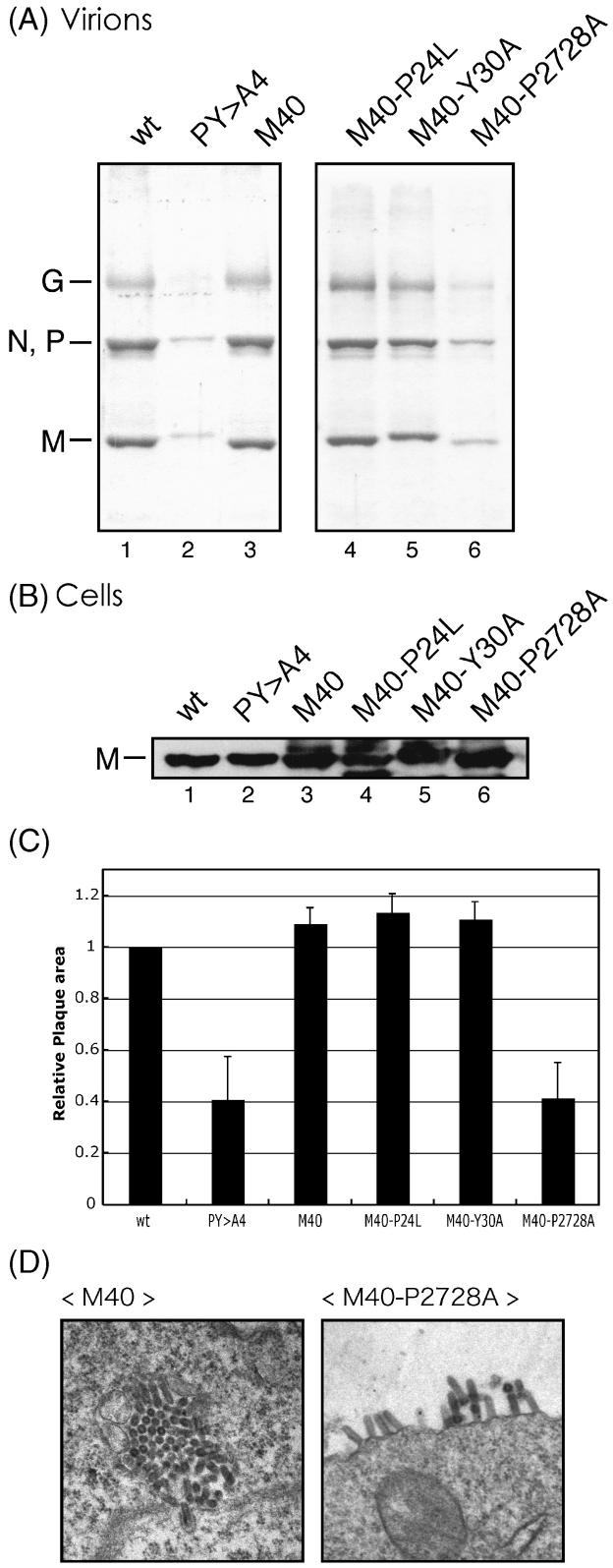

Fig. 2. Characterization of VSV recombinants by protein profiles, plaque area, and electron microscopy. (A) SDS–PAGE analysis of virion proteins from virions released from BHK-21 cells at 8 h post-infection. The G, N/P, and M proteins are indicated for VSV-WT (lane 1), PY > A4 (lane 2), M40-WT (lane 3), M40-P24L (lane 4), M40-Y30A (lane 5), and M40-P2728A (lane 6). The L protein is not shown. (B) SDS–PAGE analysis of M protein levels in cells infected with the indicated virus. (C) The relative plaque areas for VSV-WT, PY > A4, M40-WT, M40-P24L, M40-Y30A, and M40-P2728A are shown as a bar graph. The average plaque area for VSV-WT was set at 1.0. The bars represent an average of multiple plaque area calculations using BHK-21 cells. (D) Representative electron micrographs of M40-WT- and M40-P2728A-infected BHK-21 cells.

was packaged into budding virions (Fig. 3A). As expected, endogenous tsg101 was not detected at appreciable levels in VSV-WT virions (Irie et al., 2004a); however, tsg101 was readily detected in M40-WT virions (Fig. 3A, compare lanes 1 and 2). Interestingly, tsg101 was also detected in the M40-Y30A recombinant (lane 4), but was not present in the PTAP-deficient M40-P24A and M40-P2728A recombinants (Fig. 3A, lanes 3 and 5). Similar results were obtained using human 293T and HeLa cells (data not shown).

To prove that endogenous tsg101 was indeed packaged within the virus particles, purified M40-WT virions were treated with detergent alone, trypsin alone, or detergent plus trypsin (Fig. 3B). As expected, tsg101 was completely degraded when virions were treated with both TX-100 and trypsin (lane 4). In contrast, tsg101 was not degraded in the presence of trypsin alone (lane 2) or TX-100 alone (lane 3). The M protein of VSV was used as an internal virion protein control under identical conditions (Fig. 3B, lanes 5–8). Thus, endogenous tsg101 is indeed incorporated into budding virions, and there is a strict correlation between incorporation of specific host proteins into budding virions and the type of functional L-domain present in the viral matrix protein.

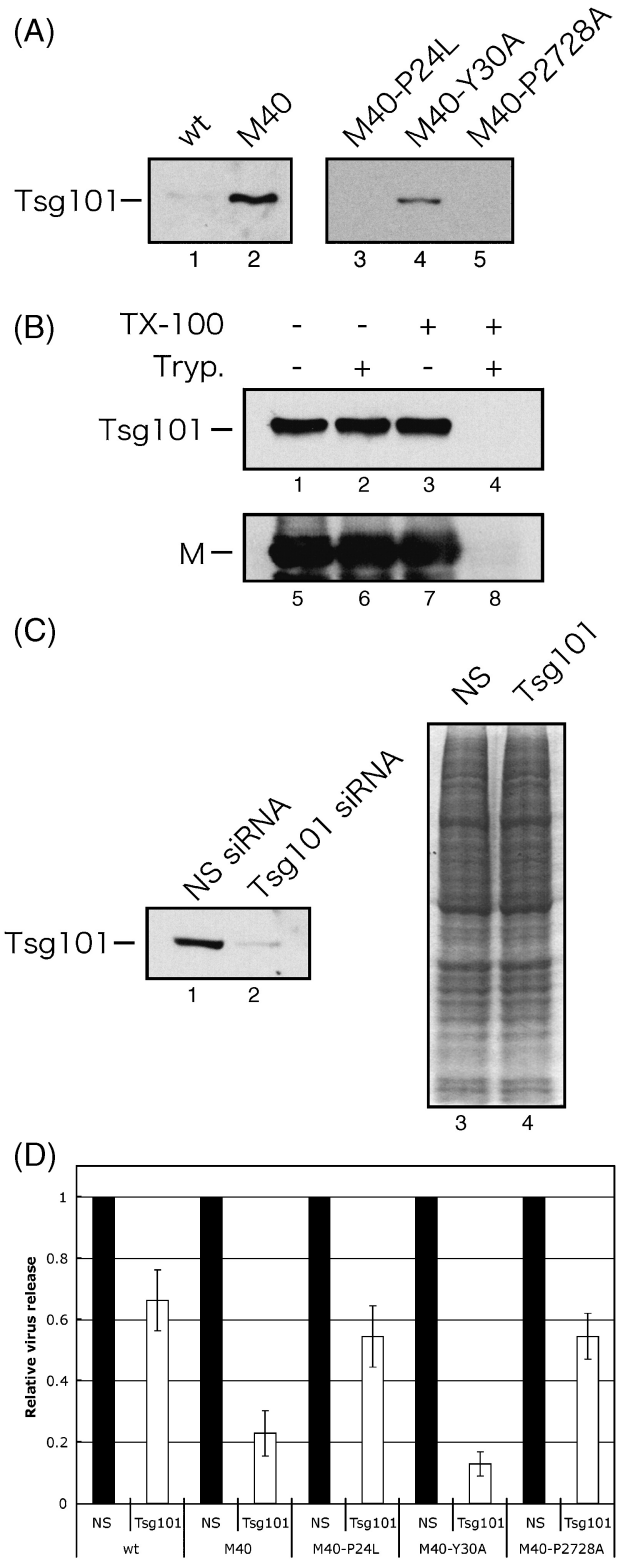

Fig. 3. Packaging of endogenous tsg101 into virions. Western blot using anti-tsg101 antiserum to detect endogenous tsg101 packaged into VSV-WT (lane 1), M40-WT (lane 2), M40-P24L (lane 3), M40-Y30A (lane 4), and M40-P2728A (lane 5) virions released from BHK-21 cells. (B) Protease protection assay. Purified virions were either untreated (lanes 1 and 5), treated with trypsin alone (lanes 2 and 6), TX-100 alone (lanes 3 and 7), or TX-100 and trypsin (lanes 4 and 8). The presence of endogenous tsg101 (lanes 1–4) or VSV M (lanes 5–8) was determined by Western blot. (C) Western blot demonstrating that endogenous tsg101 expression is inhibited following transfection of tsg101-siRNA (lane 2), but is not inhibited following transfection of NS-siRNA (lane 1). Coomassie blue stain of total protein extract from NS-siRNA-transfected cells (lane 3) and tsg101-siRNA-transfected cells (lane 4). (D) tsg101 siRNA inhibits budding of PTAP-containing recombinants. Human 293T cells were first transfected with tsg101-specific siRNA or a non-specific (NS) siRNA, and then infected with VSV (wt), M40-WT, M40-P24L, M40-Y30A, or M40-P2728A. Virion release in the presence of NS siRNA was set at 1.0 for all viruses. Each white bar represents an average of at least three independent experiments.

Functional role of tsg101 in budding of VSV M40 recombinants

We next sought to determine whether incorporation of host proteins into budding virions does indeed correlate with a functional relevance for efficient budding. Toward this end, expression of endogenous tsg101 in human 293T cells was inhibited by transfection of siRNAs specific for tsg101. A non-specific (NS) siRNA was transfected in an identical manner and served as a negative control. Transfection of tsg101 siRNA (Fig. 3C, lane 2), but not of NS siRNA (lane 1), was shown to inhibit expression of tsg101 in 293 cells that were subsequently infected with virus. Identical protein profiles of total cell extracts from NS-siRNA- and tsg101-siRNA-transfected cells were observed following staining with Coomassie blue (Fig. 3C, lanes 3 and 4, respectively). Human 293T cells were transfected with tsg101 or NS siRNA twice, followed by infection with the indicated virus (Fig. 3D). The titer of each virus in the presence of NS siRNA was set at 1.0 (Fig. 3D). As expected, titers of VSV-

WT were reduced < 2.0-fold when tsg101 expression was inhibited (Fig. 3D), indicating that this PPPY-containing virus is not dependent on tsg101 expression for efficient budding. In contrast, titers of M40-WT were reduced by approximately 5.0-fold in the presence of tsg101 siRNA as compared to those in the presence of NS siRNA (Fig. 3D). Similarly, titers of M40-Y30A were reduced by > 5.0-fold in the presence of tsg101 siRNA compared to those in the presence of NS siRNA (Fig. 3D). Lastly, titers of both M40-P24L and M40-P2728A were reduced < 2.0-fold in the presence of tsg101 siRNA (Fig. 3D). These results demonstrate that recombinants possessing a functional PTAP type L-domain were more sensitive to depletion of tsg101 than those viruses possessing a functional PPxY type L-domain. Of interest is the finding that M40-WT was sensitive to depletion of tsg101, although this recombinant possesses both a PTAP and a PPxY L-domain. These data indicate that the short L-domain sequence from Ebola virus is enough to re-direct the budding pathway of infectious VSV to one that is dependent on tsg101 and presumably other ESCRT proteins for efficient release.

Packaging of Nedd4 into VP40 VLPs and recombinant viruses

The PPxY L-domain is known to mediate interactions with cellular ubiquitin ligases through their WW-domains. Previous work in our laboratory demonstrated that VP40 could interact in vitro with the yeast Rsp5 protein (Nedd4 homolog), a ubiquitin ligase with multiple WW-domains (Harty et al., 2000). To demonstrate further that such an interaction could occur in vivo, we examined the ability of VP40 to recruit ubiquitin ligases into VLPs. Cells were transfected with ubiquitin ligases Nedd4 or AIP4 in the absence (top panels) or presence (bottom panels) of VP40 (Fig. 4A). VLPs were harvested from the culture media by pelleting through a sucrose cushion and subsequent flotation on a discontinuous sucrose gradient. Under these conditions, VP40 VLPs have been shown to partition in upper fractions 2 and 3 (Licata et al., 2004). Neither Nedd4 nor AIP4 was detected in any VLP fraction in the absence of VP40 (Fig. 4A, top panels). However, in cells co-expressing VP40, Nedd4 was detected in purified VLPs (Fig. 4A, bottom panel, lane 2), whereas AIP4 was not. These data indicate that VP40 can recruit Nedd4 into VLPs and that recruitment of Nedd4 is specific, as the related family member, AIP4, was excluded from VP40 VLPs (Fig. 4A, bottom panel, lane 2).

We next sought to determine whether the M40 recombinants possessing different L-domain motifs would interact with and package Nedd4 into infectious virus. As described above for tsg101, BHK-21 cells were infected with VSV-WT, PY > A4, or the M40 recombinants, and equivalent amounts of virions were harvested at 8 h post-infection. Antiserum against endogenous Nedd4 was used to detect Nedd4 in budding virions (Fig. 4B). Indeed, endogenous

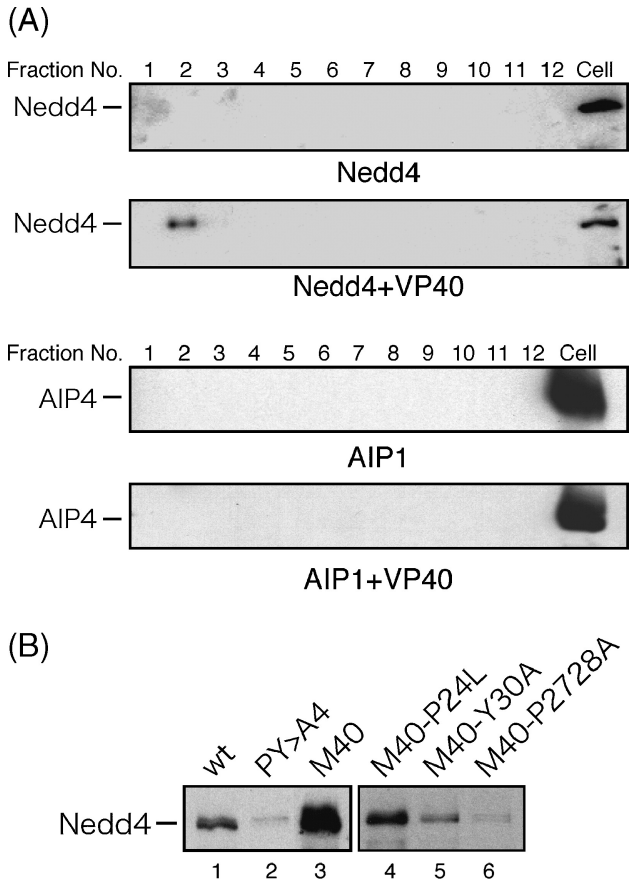

Fig. 4. (A) Human 293T cells were transfected with Nedd4 or AIP4 in the absence (top panels) or presence (bottom panels) of VP40-WT. VLPs were floated on a discontinuous sucrose gradient and equivalent fractions from the top (#1) to bottom (#12) of the gradient were analyzed for the presence of Nedd4 or AIP4 by Western blotting. As a control, cell lysates (Cell) from each condition were analyzed similarly to demonstrate expression of Nedd4 and AIP4 in cells. (B) Western blot using anti-Nedd4 antiserum to detect endogenous Nedd4 packaged into VSV-WT (lane 1), PY > A4 (lane 2), M40-WT (lane 3), M40-P24L (lane 4), M40-Y30A (lane 5), and M40-P2728A (lane 6) virions released from BHK-21 cells.

Nedd4 was detected in VSV-WT (Fig. 4B, lane 1), but was not detected at an appreciable level in the PY > A4 recombinant (lane 2). Interestingly, Nedd4 was packaged abundantly in M40-WT (lane 3) and in the M40-P24L recombinant (lane 4). Both of these viruses possess an intact PPEY motif. Conversely, the level of Nedd4 packaged into recombinants M40-Y30A (lane 5) and M40-P2728A (lane 6) was significantly lower than that packaged into M40-WT and M40-P24L. As described above for tsg101, there is good correlation between incorporation of endogenous Nedd4 into budding virions and the type of functional L-domain present in the viral matrix protein.

Discussion

The precise mechanism by which viral L-domains and host protein interactions mediate efficient budding remains

to be determined. While the Ebola virus VP40 VLP budding assay has revealed much useful information regarding the molecular aspects of VP40 budding (Irie et al., 2004b; Kolesnikova et al., 2002; Licata et al., 2003, 2004; Martin-Serrano et al., 2001; Noda et al., 2002; Swenson et al., 2004; Timmins et al., 2001, 2003; Yasuda et al., 2003), functional characterization of these Ebola sequences in the context of a virus infection is essential, since differences in L-domain function may exist between a VLP budding assay and a virus infection. We hypothesized that the VSV model system would be ideal for studying the L-domain function of a BSL-4 pathogen such as Ebola virus. For example, insertion of the Ebola virus L-domain in place of that of VSV M resulted in a 10- to 12-fold enhancement of VLP budding (Irie et al., 2004b). In contrast, a similar budding advantage was not observed in this report when the identical Ebola virus L-domain was engineered into the VSV genome to yield the M40-WT recombinant. It is possible that the M40-WT recombinant may have a budding advantage over VSV-WT in a cell type other than BHK-21 cells, or perhaps that the Ebola virus L-domains are not as efficient in the context of a VSV infection. Interestingly, preliminary data indicate that the M40-WT recombinant buds from a mosquito cell line at 100- to 1000-fold higher titers than VSV-WT (Irie and Harty, unpublished data). It will be of interest to determine whether this enhancement is due solely to the insertion of Ebola virus L-domain sequences.

Earlier studies by our group demonstrated that each L-domain motif within VP40 possesses L-domain activity alone in a VLP budding assay (Licata et al., 2003). In this report, we expanded on these findings by demonstrating that each of the Ebola virus L-domain motifs alone was functional in the context of a VSV infection. Indeed, recombinants possessing a mutation in either the PTAP (M40-P24L) or PPEY (M40-Y30A) motif were able to bud as well as M40-WT and VSV-WT in BHK-21 cells. In contrast, the double mutant (M40-P2728A) was defective in budding due to the lack of L-domain activity. It should be noted that insertion of the Ebola virus L-domain sequence into the VSV genome did not adversely affect synthesis of M protein or virion morphology as determined by immunoprecipitation and electron microscopy.

The Ebola virus L-domain sequence not only was able to function in the context of a VSV infection, but also was able to redirect budding of VSV into a tsg101-dependent pathway. Indeed, the presence of the Ebola virus PTAP motif and flanking amino acids within the VSV M protein allowed for an interaction with endogenous tsg101 and packaging of this host protein into budding virions. Importantly, the PTAP-containing M40 recombinants were functionally dependent on tsg101 expression for efficient release as demonstrated by siRNA techniques. Interestingly, budding of M40-WT was reduced to a level similar to that of M40-Y30A in the presence of tsg101 siRNA. This finding suggests that the Ebola virus PTAP L-domain motif in M40-WT may be more dominant than the PPEY motif, even though the PPEY motif possesses L-domain activity alone in recombinant M40-P24L. In addition to tsg101, endogenous Nedd4 was found to be packaged specifically into VP40 VLPs and efficiently into VSV recombinants possessing an intact PPxY motif. The ability of VSV or VSV recombinants to utilize other members of the ESCRT machinery for efficient budding remains to be determined. Increasing evidence suggests that non-PTAP-containing retroviruses also utilize the ESCRT machinery for budding (Demirov and Freed, 2004; Kikonyogo et al., 2001; Martin-Serrano et al., 2003, 2005; Strack et al., 2003).

It is intriguing that the 15-amino-acid L-domain region of Ebola virus was sufficient to modify the budding pathway of VSV from a tsg101-independent pathway to a tsg101-dependent pathway. Thus, VSV represents a realistic and valuable model system for comparing and contrasting the mechanisms by which the various types of L-domains promote budding. We are in the process of using reverse-genetics to recover additional VSV recombinants possessing L-domain regions from various human pathogens, and we hope to utilize these recombinants to elucidate the role of both viral and host determinants of budding.

Materials and methods

Cells, viruses, and antibodies

BHK-21 and human 293T cells were maintained in Dulbecco's minimum essential medium (DMEM; Life Technologies, Rockville, MD) supplemented with 10% fetal bovine serum (Life Technologies) and penicillin-streptomycin (Life-Technologies). All VSV recombinants and a recombinant Vaccinia virus (VvT7) were propagated in BHK-21 cells. All virus stocks were titrated by standard plaque assay on BHK-21 cells. Monoclonal antibody (mAb) 23H12 specific for the M protein of VSV (Indiana) was kindly provided by D.S. Lyles (Wake Forest University, School of Medicine, Winston-Salem, NC). A plasmid encoding AIP4 was kindly provided by R. Longnecker (Northwestern Univ., Illinois). Anti-tsg101 mAb (4A10; Gene Tex) and anti-Nedd4 pAb (BD PharMingen) were used according to the protocols of the suppliers.

Construction and recovery of VSV recombinants

Plasmid pVSV-FL encoding full-length VSV cDNA (Indiana serotype) was kindly provided by J.K. Rose (Yale University School of Medicine, New Haven, CT). Construction of the chimeric M40 gene was described previously (Irie et al., 2004b), and mutations were introduced into the M40 gene using a standard PCR technique to yield M40-P24L, M40-Y30A, and M40-P2728A genes. These chimeric genes were inserted back into pVSV-FL to generate M40-WT, M40-P24L, M40-Y30A, and M40-P2728A recombinant viruses.

Virion protein profiles

BHK-21 cells in 6-well plates were infected with VSV recombinants at an MOI of 10. After 1-h incubation at 37 °C, inocula were removed, cells were washed with phosphate-buffered saline (PBS) three times, and then incubated in serum-free DMEM at 37 °C for 8 h. Culture medium was harvested and clarified at 3000 rpm for 10 min. Virions were then centrifuged at 36,000 rpm for 2.5 h through a 20% sucrose cushion. The pellet was suspended in SDS–PAGE sample buffer (125 mM Tris–HCl [pH 6.8], 4.6% sodium dodecyl sulfate [SDS], 10% 2-mercaptoethanol, 0.005% bromophenol blue, 20% glycerol) and analyzed by SDS–PAGE (8%) followed by staining with GelCode Blue Stain Reagent (Pierce). Cell lysates were also prepared and analyzed by Western blotting using anti-M mAb.

One-step growth curve of VSV recombinants

BHK-21 cells in 6-well plates were infected with VSV mutants at an MOI of 10. After 1-h incubation at 37 °C, inocula were removed, cells were washed with 1 × PBS three times, and incubated with DMEM containing 10% FBS at 37 °C. At the designated time points, culture medium was harvested and titrated in duplicate by a standard plaque assay on BHK-21 cells.

Protease treatment of virions

BHK-21 cells in three 35-mm diameter dishes were infected with M40-WT virus at an MOI of 10. At 10 h p.i., the culture medium was harvested and clarified by centrifugation at 3000 rpm for 10 min. The supernatant was then centrifuged at 36,000 rpm for 2.5 h through a 20% sucrose cushion. The virion pellet was suspended into 200 μl of 1 × PBS. 50 μl of the suspension was incubated with trypsin (10 μg/ml) or PBS in the presence or absence of 0.01% Triton X-100 at 37 °C for 2 h. Samples were then mixed with 3 × SDS–PAGE sample buffer, boiled, and subjected to SDS–PAGE followed by Western blotting using antibodies specific for tsg101 or VSV M.

VP40 VLP floatation gradient

Human 293T cells were transfected with plasmids expressing either c-*myc*-tagged Nedd4 or flag-tagged AIP4. At 48 h p.t., culture medium was harvested and VLPs isolated through a 20% sucrose cushion. Resuspended VLPs were then floated on a discontinuous sucrose gradient (80%, 50%, and 10%) by centrifugation at 36,000 rpm for 18 h. Twelve 1-mL fractions were taken from the top to bottom of the gradient and proteins were isolated by TCA precipitation and resuspended in 1 × Laemmli sample buffer. Transfected cells were lysed in RIPA buffer (50 mM Tris [pH 8.0], 150 mM NaCl, 1% NP-40, 0.5% deoxycholate, 0.1% sodium dodecyl sulfate [SDS]). Proteins were separated by SDS–PAGE and transferred to nitrocellulose membranes for Western blotting. Proteins were visualized by chemiluminescence and autoradiography.

Determination of plaque size

Briefly, BHK-21 cells in 100-mm dishes were infected to yield approximately 50 plaques per dish. At 24 h p.i., cells were stained with crystal violet and the area of 10 plaques on each plate was measured using NIH Image 1.52 software.

Detection of endogenous tsg101 and Nedd4 in virions

Virion samples were prepared as described above. Virion samples were subjected to SDS–PAGE (8%), followed by Western blotting using anti-tsg101 mAb and anti-Nedd4 pAb. Virion samples were also applied to SDS–PAGE (8%), followed by staining by GelCode reagent to confirm that equivalent amounts of virion proteins were utilized in this experiment.

siRNA transfection and VSV infection

siRNA transfection and VSV infection were performed as described previously (Irie et al., 2004b). Briefly, human 293T cells cultured in 6-well plates were transfected with a combination of 0.2 μg of tsg101-specific (5′-AAC CTC CAG TCT TCT CTC GTC-3′) or non-specific (NS) siRNA (5′-NNA-TTG-TAT-GCG-ATC-GCA-GAC-3′) (Dharmacon Inc.) using Lipofectamine 2000 (Invitrogen). At 24 h p.t., cells were transfected a second time in an identical manner. After 12 h, cells were infected with VSV at an MOI of 0.01. At 6 h p.i., culture medium was harvested, and the virus yield was determined by plaque assay on BHK-21 cells. Inhibition of tsg101 expression by siRNA was confirmed by Western blotting using anti-tsg101 mAb as described previously (Irie et al., 2004b).

Acknowledgments

The authors wish to thank members of the Harty lab for fruitful discussions, J. Paragas for critical reading of the manuscript, Shiho Irie for excellent technical assistance, and Peter Bell, Director of the Cell Morphology Core, for electron microscopy. This work was supported in part by NIH grants to R.N.H.

References

Demirov, D.G., Freed, E.O., 2004. Retrovirus budding. Virus Res. 106 (2), 87–102.

Gottwein, E., Bodem, J., Muller, B., Schmechel, A., Zentgraf, H., Krausslich, H.G., 2003. The Mason–Pfizer monkey virus PPPY and PSAP motifs both contribute to virus release. J. Virol. 77 (17), 9474–9485.

Harty, R.N., Brown, M.E., Wang, G., Huibregtse, J., Hayes, F.P., 2000. A PPxY motif within the VP40 protein of Ebola virus interacts physically and functionally with a ubiquitin ligase: implications for filovirus budding. Proc. Natl. Acad. Sci. U.S.A. 97 (25), 13871–13876.

Harty, R.N., Brown, M.E., McGettigan, J.P., Wang, G., Jayakar, H.R., Huibregtse, J.M., Whitt, M.A., Schnell, M.J., 2001. Rhabdoviruses and the cellular ubiquitin–proteasome system: a budding interaction. J. Virol. 75 (22), 10623–10629.

Irie, T., Licata, J.M., Jayakar, H.R., Whitt, M.A., Bell, P., Harty, R.N., 2004a. Functional analysis of late-budding domain activity associated with the PSAP motif within the vesicular stomatitis virus M protein. J. Virol. 78 (14), 7823–7827.

Irie, T., Licata, J.M., McGettigan, J.P., Schnell, M.J., Harty, R.N., 2004b. Budding of PPxY-containing rhabdoviruses is not dependent on host proteins TGS101 and VPS4A. J. Virol. 78 (6), 2657–2665.

Jasenosky, L.D., Kawaoka, Y., 2004. Filovirus budding. Virus Res. 106 (2), 181–188.

Jayakar, H.R., Murti, K.G., Whitt, M.A., 2000. Mutations in the PPPY motif of vesicular stomatitis virus matrix protein reduce virus budding by inhibiting a late step in virion release. J. Virol. 74 (21), 9818–9827.

Kikonyogo, A., Bouamr, F., Vana, M.L., Xiang, Y., Aiyar, A., Carter, C., Leis, J., 2001. Proteins related to the Nedd4 family of ubiquitin protein ligases interact with the L domain of Rous sarcoma virus and are required for gag budding from cells. Proc. Natl. Acad. Sci. U.S.A. 98 (20), 11199–11204.

Kolesnikova, L., Bugany, H., Klenk, H.D., Becker, S., 2002. VP40, the matrix protein of Marburg virus, is associated with membranes of the late endosomal compartment. J. Virol. 76 (4), 1825–1838.

Licata, J.M., Simpson-Holley, M., Wright, N.T., Han, Z., Paragas, J., Harty, R.N., 2003. Overlapping motifs (PTAP and PPEY) within the Ebola virus VP40 protein function independently as late budding domains: involvement of host proteins TSG101 and VPS-4. J. Virol. 77 (3), 1812–1819.

Licata, J.M., Johnson, R.F., Han, Z., Harty, R.N., 2004. Contribution of ebola virus glycoprotein, nucleoprotein, and VP24 to budding of VP40 virus-like particles. J. Virol. 78 (14), 7344–7351.

Martin-Serrano, J., Zang, T., Bieniasz, P.D., 2001. HIV-1 and Ebola virus encode small peptide motifs that recruit tsg101 to sites of particle assembly to facilitate egress. Nat. Med. 7 (12), 1313–1319.

Martin-Serrano, J., Zang, T., Bieniasz, P.D., 2003. Role of ESCRT-I in retroviral budding. J. Virol. 77 (8), 4794–4804.

Martin-Serrano, J., Eastman, S.W., Chung, W., Bieniasz, P.D., 2005. HECT ubiquitin ligases link viral and cellular PPXY motifs to the vacuolar protein-sorting pathway. J. Cell Biol. 168 (1), 89–101.

Noda, T., Sagara, H., Suzuki, E., Takada, A., Kida, H., Kawaoka, Y., 2002. Ebola virus VP40 drives the formation of virus-like filamentous particles along with GP. J. Virol. 76 (10), 4855–4865.

Ott, D.E., Coren, L.V., Sowder II, R.C., Adams, J., Nagashima, K., Schubert, U., 2002. Equine infectious anemia virus and the ubiquitin–proteasome system. J. Virol. 76 (6), 3038–3044.

Panchal, R.G., Ruthel, G., Kenny, T.A., Kallstrom, G.H., Lane, D., Badie, S.S., Li, L., Bavari, S., Aman, M.J., 2003. In vivo oligomerization and raft localization of Ebola virus protein VP40 during vesicular budding. Proc. Natl. Acad. Sci. U.S.A. 100 (26), 15936–15941.

Perez, M., Craven, R.C., de la Torre, J.C., 2003. The small RING finger protein Z drives arenavirus budding: implications for antiviral strategies. Proc. Natl. Acad. Sci. U.S.A. 100 (22), 12978–12983.

Puffer, B.A., Parent, L.J., Wills, J.W., Montelaro, R.C., 1997. Equine infectious anemia virus utilizes a YXXL motif within the late assembly domain of the Gag p9 protein. J. Virol. 71 (9), 6541–6546.

Schmitt, A.P., Lamb, R.A., 2004. Escaping from the cell: assembly and budding of negative-strand RNA viruses. Curr. Top. Microbiol. Immunol. 283, 145–196.

Schmitt, A.P., Leser, G.P., Waning, D.L., Lamb, R.A., 2002. Requirements for budding of paramyxovirus simian virus 5 virus-like particles. J. Virol. 76 (8), 3952–3964.

Strack, B., Calistri, A., Craig, S., Popova, E., Gottlinger, H.G., 2003. AIP1/ALIX is a binding partner for HIV-1 p6 and EIAV p9 functioning in virus budding. Cell 114 (6), 689–699.

Swenson, D.L., Warfield, K.L., Kuehl, K., Larsen, T., Hevey, M.C., Schmaljohn, A., Bavari, S., Aman, M.J., 2004. Generation of Marburg virus-like particles by co-expression of glycoprotein and matrix protein. FEMS Immunol. Med. Microbiol. 40 (1), 27–31.

Timmins, J., Scianimanico, S., Schoehn, G., Weissenhorn, W., 2001. Vesicular release of ebola virus matrix protein VP40. Virology 283 (1), 1–6.

Timmins, J., Schoehn, G., Ricard-Blum, S., Scianimanico, S., Vernet, T., Ruigrok, R.W., Weissenhorn, W., 2003. Ebola virus matrix protein VP40 interaction with human cellular factors Tsg101 and Nedd4. J. Mol. Biol. 326 (2), 493–502.

von Schwedler, U.K., Stuchell, M., Muller, B., Ward, D.M., Chung, H.Y., Morita, E., Wang, H.E., Davis, T., He, G.P., Cimbora, D.M., Scott, A., Krausslich, H.G., Kaplan, J., Morham, S.G., Sundquist, W.I., 2003. The protein network of HIV budding. Cell 114 (6), 701–713.

Yasuda, J., Nakao, M., Kawaoka, Y., Shida, H., 2003. Nedd4 regulates egress of Ebola virus-like particles from host cells. J. Virol. 77 (18), 9987–9992.